Project Acronym: MuG

Project title: Multi-Scale Complex Genomics (MuG)

Call: H2020-EINFRA-2015-1

Topic: EINFRA-9-2015

Project Number: 676556

Project Coordinator: Institute for Research in Biomedicine (IRB Barcelona)

Project start date: 1/11/2015

Duration: 36 months

Deliverable 7.1: Report on the use of MuG VRE on the senescence project

Lead beneficiary: Centre National de la Recherche Scientifique (CNRS)

Dissemination level: PUBLIC

Due date: 31/10/2018

Actual submission date: 21/11/2018

This project has received funding from the European Union's Horizon 2020 research and innovation programme under grant agreement No 676556.

Document history

Version	Contributor(s)	Partner	Date	Comments
0.1	Satish Sati	CNRS	05/11/2018	First draft
0.2	François Serra, David Castillo	CRG	07/11/2018	Revision and additions
0.3	Satish Sati	CNRS	19/11/2018	Final draft
1.0			20/11/2018	Final version. Approved by Supervisory Board

Table of contents

Executive summary

We have generated high resolution 3D chromatin maps from acute (oncogene-induced) and chronic (replicative senescence) senescent cells. Although both differ in their mode of initiation and their relevant outputs (tumour suppression and aging respectively), both display a loss in short range contacts and a gain in long range contacts. However at the level of genome compartments, they show opposite behaviour. While the changes in oncogene senescence was driven by heterochromatin interactions leading to strong compartmentalisation, the replicative senescence display a loss of compartmentalisation due to decrease in intra euchromatin interactions. Further, we were able to identify the regions that form heterochromatin bodies in oncogene senescence and termed them as senescence associated heterochromatin domains. Experiments and physical modelling show that the release of these regions from the nuclear lamina and gain in inter-SAHD interactions were the key driver of oncogene-induced senescence, whereas no release from the lamina is observed in replicative senescence.

1 INTRODUCTION

Previous studies employing both acute and chronic senescent systems have showed that senescence in general is associated with global chromatin reorganisation (*1-5*). As chronic senescence takes time to set in (replication induced senescence, RIS), in our experiments we used acute senescent system (oncogene induced senescence, OIS) to follow chromatin changes over a time course. We employ serial passaging of WI38 primary fibroblasts as replicative senescent model and WI38 cells overexpressing the RAF oncogene (WI38hTERT/ GFPRAF1ER immortal cells) as an oncogene-induced senescence system (*6*). At CNRS-IGH, we performed Hi-C, RNA-Seq and WGBS experiments. Hi-C was performed in replicates with each replicate being sequenced over 400 million reads, giving a total of 800 million reads per time point. For the same cells, RNA-Seq was performed where, ~40 million paired-end reads were generated per replicate (done in triplicates).

2 Differences in 3D genome organization

We selected OIS D0, D2, D6 and D10 (days upon OIS induction) as time points for our Hi-C experiments. In the RIS system we used proliferative and replicative senescent cells. The Hi-C assays were done on FACS-sorted populations in the G1 phase of the cell cycle, in order to keep the population homogenous. The Hi-C experiment was done in replicates with each replicate being sequenced over 400 million reads, giving a total of 800 million reads per time point. In total we have analysed ~3.3 billion chromatin interaction points across all samples. The analysis was done in parallel using external tools and TADbit. The comparison of the results between methodologies and experiments helped to standardize the analysis proposed in the VRE. Each of the step of the analysis were collated into individual modules allowing a complete transparency and intercompatibility with other tools or pipelines along all the stage of the Hi-C data analysis. The details of different TADbit modules used in Hi-C analysis are mentioned in deliverable 6.4.

Hi-C profiles of individual chromosomes display a progressive global reorganisation in OIS, with a huge gain in long range contacts, which are more prominent by D4 (by this time SAHFs are formed) (*6*) (Figure 1). These long range far cis interactions were also found in replicative senescent cells, but were confined to individual chromosome arms.

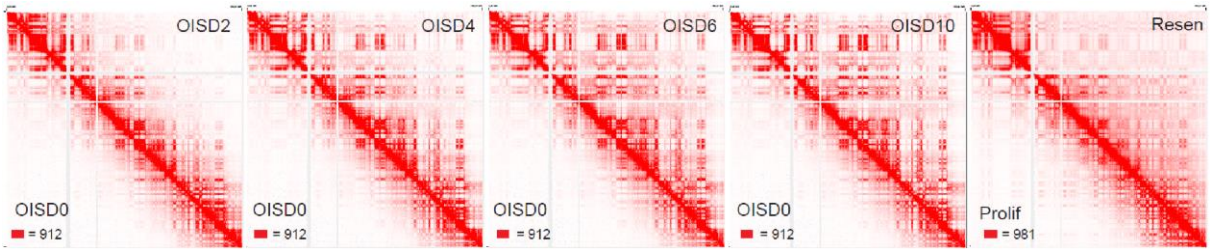

Figure 1. Hi-C maps of chromosome 5 from oncogene senescence system (OIS) and replicative senescent system (Prolif = Proliferative and Resen = replicative senescent).

Along with WP3 and WP6, we identified TADs (topologically associating domains). As described in previous studies employing several different cell types and species, we also find TADs to be conserved along the OIS and RIS states (*7*). Since the OIS genome shows strong microscopic compartmentalisation with inactive or heterochromatin regions falling in SAHFs and other regions outside SAHFs, we analyzed the changes in compartment interaction. Compartments were called using the TADbit tools installed in the VRE. The methodology based on the computation of the first eigenvector of the chromosomic correlation matrix is directly inspired from (11).

Mapping the compartments over the Hi-C matrix highlights a progressive gain in B-B interaction in OIS (Figure 2). These results suggest in OIS, the BB or heterochromatin specific interactions drive the genome towards strongly compartmentalised state, which is reflected by the occurrence of SAHFs. While in RIS, the loss in AA or euchromatin specific interactions drive the genome towards a weakly compartmentalised state.

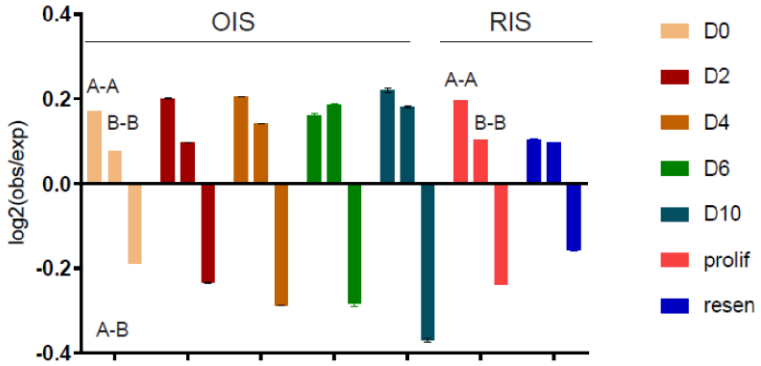

Figure 2. Mapping chromatin interactions in intra and Inter – chromatin compartments across OIS and RIS system.

To confirm these results we adopted a complementary approach in which we plot the log ratio of observed versus expected contacts between 100 kb genomic bins ranked on their eigenvector value. The results show a gain in compartmentalisation in OIS and loss in RIS.

3 Changes in 3D vs transcription

For the above mentioned cells in RIS and OIS, RNA-Seq was performed, where ~40 million paired end reads were generated per replicate (done in triplicates). Following which we analysed the correlation between the changes in compartment vs gene expression. The change in compartments was weakly associated with transcriptional changes in RIS but not associated in OIS. As active transcription start sites (TSS) are known to be more insulated, we analyzed the normalised insulation scores at active and inactive TSS (*8*). The active TSS lose insulation potential during OIS progression from OISD0 to D10, while there was a gain in insulation at these sites in RIS. Furthermore, active TSSs gain far cis inter-TAD interactions, which might be due to the SAHF formation as RIS (in the absence of SAHF formation) displays a loss in active TSS interactions.

4 Senescent Associated Heterochromatin Domains (SAHD)

As the B compartment seems to dictate the changes in OIS and it was mainly composed of H3K9me3 regions, we hypothesized that these regions might be those that form SAHFs. In order to obtain the precise coordinates of these regions, We employed the diffHiC method to get differentially interaction regions over different bin sizes (25 kb to 1mb) (10). DiffHiC analysis highlighted regions gaining interactions that are free of histone modifications except for H3K9me3. As a majority of the H3K9me3 regions are conserved across the OIS time course, we defined these conserved OIS H3K9me3 regions as Senescence associated heterochromatin domains (SAHDs). SAHDs lose intra-Domain interactions and gain inter-Domain interactions in OIS. In RIS they follow the same trend, but to a much lesser extent (Figure 3).

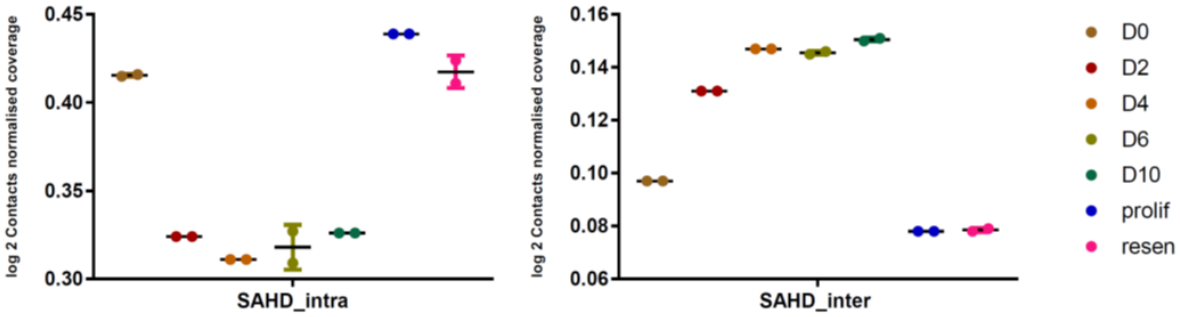

Figure 3. SAHDs lose intra domain contacts and gain long range inter domain contacts in OIS.

We hypothesized that SAHFS might be generated by the release of SAHDs from the lamina and by a loss of internal chromatin interactions, which might lead to a gain in inter-SAHD interactions. As SAHDs are poor in cytosine methylation, we performed the WGBS assay on OIS D0, D2, D6 and WI38 Proliferative, replicative senescent cells (~360 million paired end: 180 million per replicate) at CNAG Barcelona. The analysis revealed that the SAHDs were and remain poor in cytosine methylation in OIS and RIS, although there were few other regions in the genome that were differentially methylated in OIS and RIS.

To visualise SAHD interactions, WP3 members produced TADbit models at 200kb resolution for chromosome 5, from Hi-C matrices of OIS D0, D2, D4, D6, D10, WI38 proliferative and WI38 replicative senescent cells (*9*). The Hi-C interaction matrices corresponding to chromosome 5 were extracted and translated into distance restraints to be applied between each pair of particles of a 3D model. Each particle representing a 200kb bin of the input matrix. Starting from a thousand different random initial configurations, TADbit optimizes the satisfactions of the restraints through successive random displacements of the particles (12). The final conformations will each satisfy a different proportion of the total input restraints. Generated 3D models are then clustered according to structural similarities, and each of these cluster represents a different sub-population of cells in the original Hi-C experiment.

The models were then visualised in MUG VRE (Figure 4).

Figure 4. TADbit model of Chromosome 5 at 200kb resolution from OISD6 samples. The upper panel displays the 3D model and the corresponding Hi-C data. The bottom left panel displays the RNASeq data from the same cells and from control cells (OISD0).

Four regions (3 SAHD and one Non-SAHD) were chosen for 3D-FISH assay. 3D FISH analysis on OIS D0 and D6 highlights the colocalization of SHADs inside the SAHFs (Figure 5), validating our hypothesis on SAHF formation.

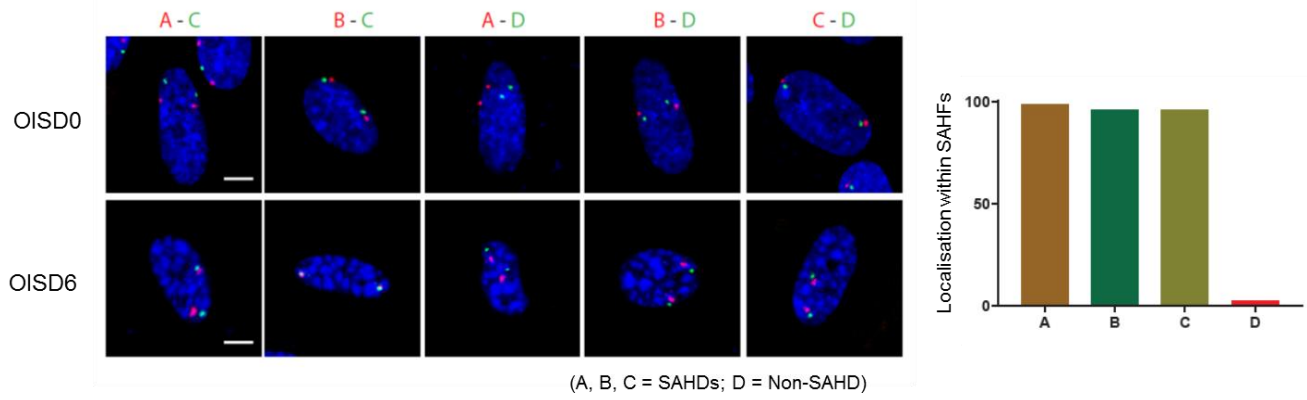

Figure 5. FISH results. The lefthand panel displays representative images from the respective FISH assay. The right hand graph displays the percent localisation of the probe regions within SAHFs in OISD6 samples.

Furthermore, we validated that SAHDs move away from periphery, their area increases (suggesting de-compaction) and the distances between the SAHDs becomes shorter in OIS. Similar FISH analysis in proliferative and RIS, displays no significant change in the distance between SAHDs, partial displacement from periphery and partial decompaction. These analysis for the target regions were also performed by *in silico modelling*. When distance distribution between the regions were computed from the TADbit models (WP3), a positive

correlation was obtained between the FISH data and TADbit models. At present WP7.1 is working with WP3 to calibrate the TADbit model such that the distances from the TADbit model can be expressed in the same unit (micrometer) as the FISH distances.

The VRE presents a unique environment to run complex Hi-C analysis. We were able to use it to perform Hi-C data normalisation and get 3D features like compartments and TADs from it. We are in process to publish these results and soon after publication these model will be kept in the public domain in VRE for future training events.

5 REFERENCES

1. L. Sun, R. Yu, W. Dang, Chromatin Architectural Changes during Cellular Senescence and Aging. *Genes (Basel)* **9**, (2018).
2. T. Chandra *et al.*, Global reorganization of the nuclear landscape in senescent cells. *Cell Rep* **10**, 471-483 (2015).
3. T. Chandra *et al.*, Independence of repressive histone marks and chromatin compaction during senescent heterochromatic layer formation. *Mol Cell* **47**, 203-214 (2012).
4. S. W. Criscione *et al.*, Reorganization of chromosome architecture in replicative cellular senescence. *Sci Adv* **2**, e1500882 (2016).
5. A. Zirkel *et al.*, HMGB2 Loss upon Senescence Entry Disrupts Genomic Organization and Induces CTCF Clustering across Cell Types. *Mol Cell* **70**, 730-744 e736 (2018).
6. M. Jeanblanc *et al.*, Parallel pathways in RAF-induced senescence and conditions for its reversion. *Oncogene* **31**, 3072-3085 (2012).
7. J. R. Dixon *et al.*, Topological domains in mammalian genomes identified by analysis of chromatin interactions. *Nature* **485**, 376-380 (2012).
8. B. Bonev *et al.*, Multiscale 3D Genome Rewiring during Mouse Neural Development. *Cell* **171**, 557-572 e524 (2017).
9. F. Serra *et al.*, Automatic analysis and 3D-modelling of Hi-C data using TADbit reveals structural features of the fly chromatin colors. *PLoS Comput Biol* **13**, e1005665 (2017).
10. A. T. L. Lun *et al.*, diffHic: a Bioconductor package to detect differential genomic interactions in Hi-C data. *BMC Bioinformatics*, **16**(1), 258 (2015).
11. E. Lieberman-Aiden *et al.*, Comprehensive mapping of long-range interactions reveals folding principles of the human genome. *Science* **326**(5950), 289-93 (2009).
12. D. Baù *et al.*, Genome structure determination via 3C-based data integration by the Integrative Modeling Platform. *Methods*, **58**(3), 300-6 (2012).